



HAL
open science

Substitutional structures in symplectic and multi-connected flat spaces and astrophysical applications

Juan Garcia Escudero

► **To cite this version:**

Juan Garcia Escudero. Substitutional structures in symplectic and multi-connected flat spaces and astrophysical applications. *Philosophical Magazine*, 2006, 86 (06-08), pp.901-907. <10.1080/14786430500375183>. <hal-00513628>

HAL Id: hal-00513628

<https://hal.science/hal-00513628v1>

Submitted on 1 Sep 2010

HAL is a multi-disciplinary open access archive for the deposit and dissemination of scientific research documents, whether they are published or not. The documents may come from teaching and research institutions in France or abroad, or from public or private research centers.

L'archive ouverte pluridisciplinaire **HAL**, est destinée au dépôt et à la diffusion de documents scientifiques de niveau recherche, publiés ou non, émanant des établissements d'enseignement et de recherche français ou étrangers, des laboratoires publics ou privés.



HAL Authorization



Substitutional structures in symple and multi-connected flat spaces and astrophysical applications

Journal:	<i>Philosophical Magazine & Philosophical Magazine Letters</i>
Manuscript ID:	TPHM-05-May-0152.R2
Journal Selection:	Philosophical Magazine
Date Submitted by the Author:	14-Sep-2005
Complete List of Authors:	Escudero, Juan; Universidad Politécnica de Madrid, Ciencia y Tecnología Aplicadas.U.D.Matemáticas; Universidad de Oviedo, Física
Keywords:	quasicrystals, crystal geometry
Keywords (user supplied):	tilings, variable stars
<p>Note: The following files were submitted by the author for peer review, but cannot be converted to PDF. You must view these files (e.g. movies) online.</p> <p>Escudero AmesICQ-Sept-fin.tex</p>	



Substitutional structures in simply and multi-connected flat spaces and astrophysical applications

Juan García Escudero

*Departamento de Matemáticas. Universidad Politécnica de Madrid. EUIT Agrícolas.
Ciudad Universitaria, 28040 Madrid, Spain*

Abstract

Hexagonal, octagonal and dodecagonal tilings of both simply and multi-connected flat spaces in 2D are considered. The tessellations of the euclidean plane have in common arrowed prototiles, which are used for the construction of fundamental polygons for the flat torus and the Klein bottle. Non deterministic derivations in formal grammars, producing non periodic ordered structures, have been introduced recently also for the analysis of variable stars with multiple periods, like the semiregular star UW Her and the Delta-Scuti star V784 Cas. Observations of the V346 Ori light curve can be modelled with similar techniques.

1. Introduction.

Geometric constructions for the generation of several types of substitutional tilings have been introduced in [1]. Non deterministic structures can be obtained by composition of the inflation rules [2,3]. In some cases the local rearrangements of tiles are included in the inflation rules, and this property allows to compute the configurational entropy [4].

Tilings of the euclidean plane have been used for quasicrystal structure determinations. Arrowed systems of lines have been studied as the basic geometric configurations for the patterns generation (Sec.2). By changing the arrowing we obtain different types of tilings that can not be generated by the constructions already studied. Discrete substitutional structures have applications in other fields. In this work we study also tessellations of multiconnected flat manifolds like the torus and the Klein bottle. We consider the square and the hexagon as fundamental polygons and several types of hexagonal, octagonal and dodecagonal tessellations. The interest of the resulting discrete structures is motivated by recent studies in cosmic topology and quantum gravity [5,6,7]. Non periodic ordered structures can also be used for the analysis of the multiperiodicity of variable stars. Artificial light curves for the semiregular UW Herculis [8] and the δ -Scuti V784 Cassiopeiae [9] have been derived by concatenation of two sinusoidal fragments following certain word sequences. The two basic building blocks represent temporal segments in a golden ratio and the number of long and short segments in a word are also in a golden ratio. The analysis can be applied also to the δ -Scuti star V346 Orionis. In Sec.3 the model is studied from the point of view of its period analysis in order to compare with the results obtained in [10].

Table 1: Prototiles and edge inflation rules for twelve-fold symmetry.

Prototiles						
α_m	β_m	$\bar{\beta}_m$	γ_m	δ_m	$\bar{\delta}_m$	
$\langle a^0 a^0 b^1 \rangle$	$\langle b^1 a^1 c^1 \rangle$	$\langle b^0 a^0 c^0 \rangle$	$\langle b^0 b^0 d^0 \rangle$	$\langle c^1 a^0 d^0 \rangle$	$\langle c^0 a^1 d^1 \rangle$	
ϵ_m	$\bar{\epsilon}_m$	ζ_m	$\bar{\zeta}_m$	η_m	θ_m	
$\langle d^1 a^0 e^1 \rangle$	$\langle d^0 a^1 e^0 \rangle$	$\langle d^1 b^0 f \rangle$	$\langle d^0 b^1 f \rangle$	$\langle c^1 c^1 f \rangle$	$\langle c^0 b^1 e^0 \rangle$	
$\bar{\theta}_m$	λ_m	μ_m	$\bar{\mu}_m$	ν_m	$\bar{\nu}_m$	ξ_m
$\langle c^1 b^0 e^1 \rangle$	$\langle e^0 b^0 e^0 \rangle$	$\langle e^1 a^1 f \rangle$	$\langle e^0 a^0 f \rangle$	$\langle d^0 c^0 e^1 \rangle$	$\langle d^1 c^1 e^0 \rangle$	$\langle d^1 d^1 d^1 \rangle$
rules						Tiles
a^0	b^0	c^0	d^0	e^0	f	
b^0	$a^1 c^0$	$d^1 b^0$	$e^0 c^1$	$d^0 f$	$e^1 e^0$	6
c^0	$d^0 b^1$	$a^0 c^1 e^0$	$b^0 d^1 f$	$e^0 e^1 c^0$	$d^1 f d^0$	19
d^1	$e^0 c^1$	$b^1 d^0 f$	$a^1 c^0 e^1 e^0$	$d^0 f d^1 b^0$	$c^0 e^1 e^0 c^1$	6
e^1	$d^0 f$	$e^1 e^0 c^1$	$d^0 f d^1 b^0$	$a^1 c^0 e^1 e^0 c^1$	$b^1 d^0 f d^1 b^0$	6
f	ee	dfd	$ceec$	$bdfdb$	$aceeca$	12

2. Hexagonal, octagonal and dodecagonal patterns in simply and multi-connected spaces.

Several types of arrowed systems of lines have been studied in recent years in order to generate planar tessellations [1-4]. They show a variety of inflation factors: Pisot unit (PU), non unit (PNU), non Pisot (NP) and rational integers. Two systems of lines for 12-fold symmetry are:

$$x = 0, y = 0, y = x \tan(\nu\pi/12) + \Gamma_{\alpha,\nu} \tag{1}$$

system A : $\nu = 1, 2, \dots, 5$: $\Gamma_{\alpha,\nu} = -\sum_{k=1}^{\alpha} s_{7-2k}$, $\alpha = \nu, \nu = 1, 2, 3$; $\alpha = 6 - \nu, \nu = 4, 5$;

$\nu = 7, 8, \dots, 11$: $\Gamma_{\alpha,\nu} = \sum_{k=1}^{\alpha} s_{7-2k}$, $\alpha = \nu - 6, \nu = 7, 8, 9$; $\alpha = 12 - \nu, \nu = 10, 11$.

system B : $\nu = 1, 2, 3, 4$: $\Gamma_{\alpha,\nu} = -\sum_{k=1}^{\alpha} s_{6-2k}$, $\alpha = \nu, \nu = 1, 2, 3$; $\alpha = 1, \nu = 4$; $\nu = 5$: $\Gamma_{\alpha,\beta} = 0$; $\nu = 7, 8, \dots, 11$: $\Gamma_{\alpha,\nu} = \sum_{k=0}^{\alpha} s_{6-2k}$, $\alpha = \nu - 6, \nu = 7, 8, 9$; $\alpha = 11 - \nu, \nu = 10, 11$.

where $s_\nu = \sin(\nu\pi/12)$. This systems of lines produce geometric configurations containing triangles. By adding arrows to the triangle edges it is possible to generate tilings by recursive subdivision. In Tab.1 we can see, up to mirror images, the possible triangle prototiles $\langle x^k y^l z^m \rangle$ with arrowed edges x^k , where $x = a, b, c, d, e, f$ and $k \in \mathbb{Z}_2$. The edge lengths are $l_a = s_1, l_b = s_2, l_c = s_3, l_d = s_4, l_e = s_5, l_f = s_6$ and they are labelled with $k = 0$ or 1 , depending on whether the arrow orientations are anticlockwise or clockwise respectively. If the mirror image of a word w is denoted by $Mir(w)$, the projection of x^k into x by $P(x^k)$ and t is the map $t(x^k \dots y^l z^m) = x^{k+1} \dots y^{l+1} z^{m+1}$. If we choose anticlockwise orientation, the substitution rules for the edges are given in Tab.1. For a tiling with inflation factor l_z/s_1 we have

$$\phi_z(x^k) = Mir(t(\phi_z(x^{k+1}))) \quad (2)$$

and $\phi_z(f) = Mir(t(\phi_z(f)))$, therefore we do not need to put an arrow on the edge f . Only x^0 and x^1 are common edges of two adjacent tiles, therefore the fact that the tilings are face to face is equivalent to $P(\phi_z^n(x^k)) = Mir(P(\phi_z^n(x^{k+1})))$, which is a consequence of eq.(2). The arrowings for the systems of lines are not unique. In fact different arrowings give different tilings, as in the case of ϕ_c where the system A must be arrowed in a different way (compare [3]) in order to get the 19 prototiles and their inflation rules. The inflation factors $(s_2/s_1)^2, s_3/s_1, (s_4/s_1)^2, s_5/s_1, s_6/s_1$ are PU,PNU,PNU,PU and NP respectively.

A system of lines similar to system A was used in [2] for the derivation of octagonal tilings with seven prototiles (five different shapes) . The inflation factors $(s_2/s_1)^2, s_3/s_1, s_4/s_1$, with $s_\nu = \sin(\nu\pi/8)$, are PNU,PU and NP respectively. A different type of system of lines was introduced in [1] for the generation of octagonal patterns with four prototiles (three different shapes) and inflation factor s_3/s_1 . The construction was extended to six-fold symmetry in [4], where the tilings obtained have three prototiles and inflation factor 2 .

For each inflation factor, except s_d/s_1 for $2d$ -fold symmetry ($d = 4, 6$), there are at least two different tilings. When a tile appears with different arrowings (in addition to their mirror images) then it is possible to generate other patterns with edge inflation rule $Mir(t(\phi_z(x^k)))$ for each x^k . In other cases , like the dodecagonal patterns with inflation factor s_5/s_1 it is possible to get tilings with a different prototile set (13 in that case). By composing the inflation rules non deterministic structures can be derived. The resulting composite tilings are face to face. When the non deterministic structures are generated by local rearrangements of tiles included in the inflation rules, the configurational entropy can be computed as in the hexagonal and octagonal patterns derived in [1,4].

In [5,11] the authors assume a multiconnected Universe where the compact spatial sections have a volume significantly smaller than the horizon volume. The space generates multiple images of cosmic objects which are linked by the holonomy group. In order to understand this facts they look for spikes in the pair separation histogram of cosmic sources by analogy with techniques used in crystallography . On the other hand one of the research directions towards a quantum theory of gravity is dynamical triangulations. In this models the quantum spacetime is represented by a simplicial complex where each element models a region of spacetime on the order of the Planck volume (see [7] and references therein). In what follows we consider tessellations of multiconnected compact flat manifolds in 2D. A grammar description along the lines of [2] is possible and it gives an algebraic model which is non commutative, non associative, and independent of a coordinate system.

The flat 2-dimensional torus is defined by abstractly gluing opposite edges of a square (see [12] for visualisations with *Mathematica* of hexagons and other structures in the surface of the topologically equivalent torus of revolution).The Klein bottle is similar to the torus, but in this case two of the opposite sides are glued to themselves, not to each other like in the torus. The hexagonal and octagonal patterns introduced in [1,2,4] share the tile $\eta : < c^1 c^1 f >$ which appears also in some of the dodecagonal patterns in Tab.1. A tessellation for the flat torus can be obtained if we construct a square by gluing η with its mirror image $< c^0 c^0 f >$ by the edge f . The inflation rules for the edge f are palindromes and, once the opposite

edges are glued to form the torus, they share the same arrow and therefore the tiling will be face to face . The hexagon also reproduces the flat torus. The tile $\mu : < e^1 a^1 f >$ can be used for the construction of the hexagon, first by gluing with its mirror image through the edge e in order to get the isosceles triangle with edges $f, a^0 a^1, f$ and then by gluing six copies of this triangle by its edge f . For the Klein bottle the possible inflation factors are of the type s_d/s_1 for $2d$ -fold symmetry ($d = 4, 6$). For this cases the edge inflation rules are palindromes (see Tab.1 for the inflation factor s_6/s_1) and no arrows are needed in order to fulfil the face to face condition.

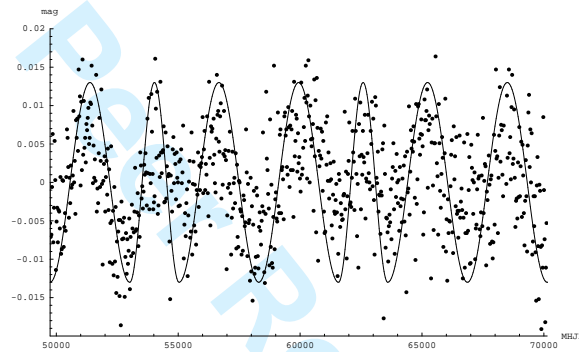


Fig.1.-V346 Ori light curve and the sequence corresponding to the first seven letters of the Fibonacci word. The ordinate is the differential stellar magnitude. The abscise is the time $MHJD = (JD - 2452218) \times 10^5$

3. Applications to variable stars with multiple periods.

Theoretical work on stellar pulsations allows to get structural information about stars interiors from variations in their brightness. We interpret the variations on the basis of 1D tilings obtained by substitution rules (see Tab.1 for 1D tilings obtained by the edge substitution rules). Semiregular variable stars are pulsating red giants with periods of a few hundred days in the case of stars with larger amplitudes. δ -Scuti stars pulsate with periods between 30 min. and 6 h. In this section Fibonacci sequences are applied to the analysis of the multiperiodicity of the δ -Scuti type variable star V346 Ori . A D0L-system $G = (\Sigma, \phi, \omega)$ can be used in order to describe the Fibonacci sequences. Σ is an alphabet, ϕ is an endomorphism defined on the set Σ^* of all the words of Σ , and ω , referred to as the axiom, is an element of Σ^* . For the Fibonacci sequence the alphabet is $\Sigma = \{L, S\}$ and $\phi : \{L \mapsto \phi(L) = LS, S \mapsto \phi(S) = L\}$. The artificial light curves are generated by

1
2
3 concatenation of two sinusoidal fragments ordered according to a Fibonacci word . The two
4 basic building blocks represent temporal segments in a golden ratio .
5

6 The observations we analyse were taken on the night of 4 November 2001 at the 1.52m
7 telescope (Loiano, Italy) . In Fig.1 are plotted the de-trended and zero averaged Johnson U
8 differential magnitudes of V346 Ori relative to HD 35351(see [10]). In the same figure we
9 can see the artificial light curve generated by applying the production rules to the axiom
10 $SL: SL \mapsto \phi^3(SL) = LSLLSLLS$. The curve is constructed by concatenation of simple
11 sinusoids with two different lengths L and S in a golden ratio τ and following the sequence
12 $\phi^3(SL)$. The temporal segments we have considered are $L = \text{MHJD } 3325$ and $S = \text{MHJD } 2055$
13 with $\text{MHJD} = (\text{JD} - 2452218) \times 10^5$ and they have been chosen by matching with the empirical
14 dataset (Fig.1).
15
16

17 The Fourier spectrum of an artificial light curve with two sinusoidal fragments with lengths
18 L and S units following a Fibonacci sequence is dense in the real line (linear combination
19 with integer coefficients of two fundamental frequencies in a golden ratio) and shows sharp
20 peaks when the word length is long enough [8,9]. The two periods corresponding to the peaks
21 with highest amplitudes have $P_1 = (3 - \tau)L$ and $P_2 = (3 - \tau)S$ units. In the data analysis
22 performed in [10] four frequencies are identified : 34.9 ± 2.2 , 23.1 ± 2.7 , 45.7 ± 2.3 , 18.3 ± 2.3 cpd
23 with amplitudes 3.9 ± 0.2 , 2.3 ± 0.2 , 1.6 ± 0.2 , 1.5 ± 0.2 respectively . The Fourier spectrum of
24 the curve corresponding to the first seven letters of $\phi^3(SL)$ shows frequencies 33.8, 24.1, 43.4
25 cpd with normalized amplitudes 1, 0.42, 0.25 while if we analyse the whole curve $\phi^3(SL)$ the
26 peaks have narrower bandwidths and they appear at frequencies 35.1, 21.9, 43.9 cpd. They
27 are in good agreement with those found in [10] except the fourth frequency which does not
28 appear in our analysis. In order to obtain the right periodicities , observations of longer
29 periods of time are needed.
30
31
32
33

34 The oscillations of the δ -Scuti star V784 Cas have been studied in [9]. The artificial light
35 curve has been generated by a non deterministic derivation in a context- sensitive grammar
36 (grammar of type 1 in the Chomsky hierarchy), containing also two sinusoidal fragments in
37 a golden ratio . The resulting dominant period of the model is similar to the one described
38 in the Hiparcos catalog, and the other frequencies are not very different in comparison with
39 those found by standard methods.
40
41
42
43
44
45
46
47
48
49
50
51
52
53
54
55
56
57
58
59
60

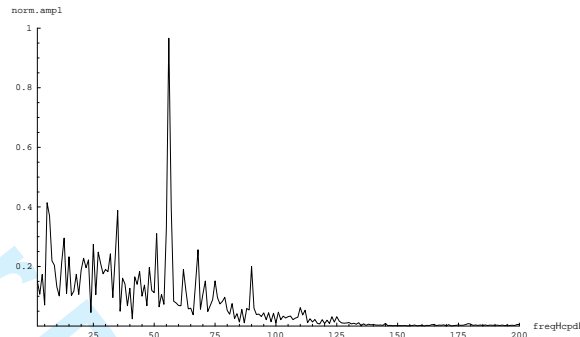


Fig.2.-Fourier spectrum for the UW Her artificial light curve with sudden amplitude changes. The analyzed interval is MJD 3892-9814 (MJD=JD-2441799). The amplitudes are normalized and the frequency is given in units of $1/5922$ cycles per day (cpd). The three peaks with the largest amplitudes correspond to the periods of 108, 174 and 1077 days

The semiregular star UW Her can be studied with the help of models based on stochastic sinusoidal sequences [8]. The analysed data were obtained by variable star observers of the British Astronomical Association. A stochastic 0L-system is a 4-tuple $G = \{\Sigma, P, \Omega, \pi\}$ where P is a set of productions r_i and $\pi : P \rightarrow (0, 1]$ is a probability distribution. We define a Fibonacci stochastic L-system with $P = \{r_1, r_2\}$ and $r_1 : \{L \mapsto LS, S \mapsto L\}, r_2 : \{L \mapsto SL, S \mapsto L\}$. The sinusoidal fragments in the model have lengths $L = 126$ and $S = 78$ days. The Fourier spectrum shows two intense peaks at 174 and 108 days. When, according to the observations, the amplitudes of some sinusoids are increased by a factor 3, then a third peak appears corresponding to a period of 1077 days (see Fig.2). These peaks are also in good agreement with those found by other methods, in spite of the fact that the analysed intervals and datasets are not the same. For generic variable stars other types of inflation factors, in addition to the golden number, should be considered. More than two buildings blocks in the underlying 1D tilings (see Tab.1 for some examples), could be necessary for the generation of the artificial light curves.

6. Concluding remarks.

In this work we have considered tilings of the euclidean plane that can be generated with the help of systems of lines which give a finite size basic triangle pattern. One way to look for inflation rules is to add arrows to the edges in the basic triangle patterns. A change in

1
2
3 the arrowings gives new tilings . Due to the variety of inflation factor types, the structures
4 have several types of Bragg spectra. In some cases deterministic and non deterministic
5 substitution rules can be used also for the generation of tessellations for the flat torus and
6 the Klein bottle.
7

8
9 Substitutional sequences have been in the basis of models for the analysis of multiperiodic
10 variable stars. The δ -Scuti star V346 Ori has been studied with the same technique, although
11 a determinstic derivation is enough due probably to the short time interval analysed. By
12 comparing with the main periodicities obtained in the Fourier analysis, the time expectations
13 for the minima in the light curve are reduced by a factor related to the golden number.
14

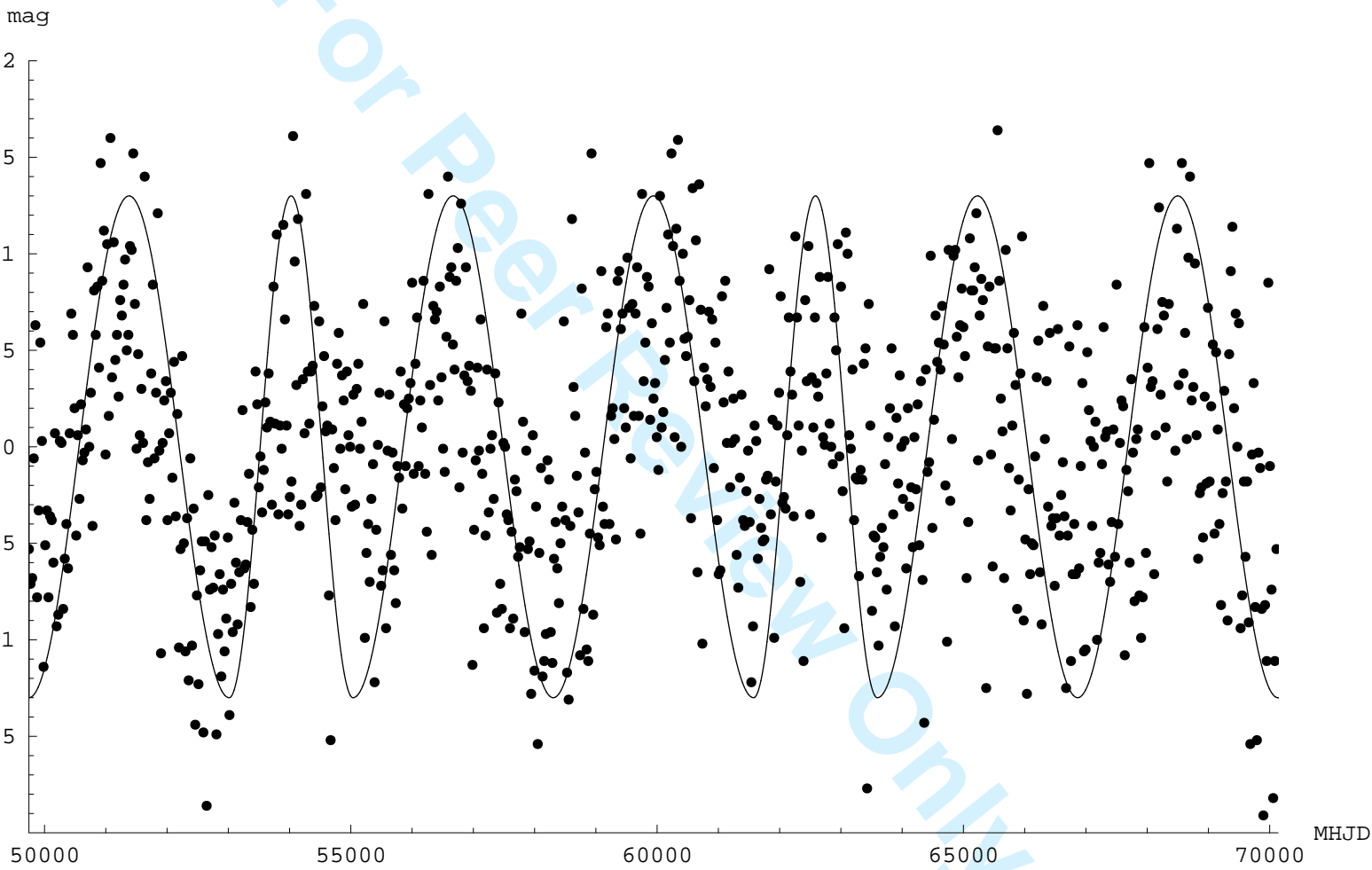
15 16 **Acknowledgements**

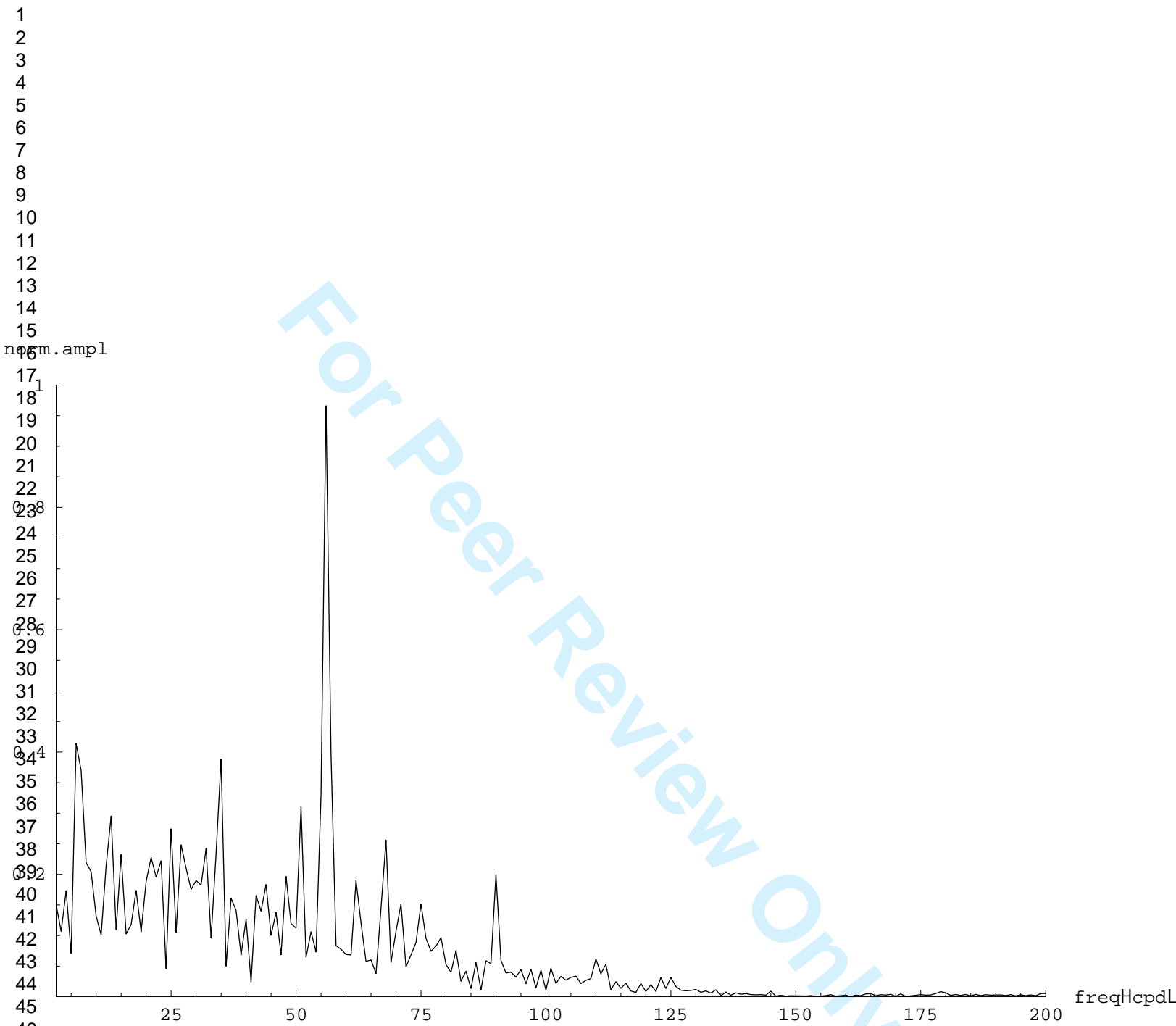
17 The NASA ADS Abstract Service and the SIMBAD database at CDS-Strasbourg, France,
18 were used to access data about V346 Ori (D.F.M.Folha) and references. I thank ICQ9
19 Committee-Ames Laboratory and Universidad Politécnica de Madrid for financial support.
20
21

22 23 **References**

- 24
25 [1] J.G. Escudero, Int. J. Mod. Phys. B. **17** 2925 (2003).
26 [2] J.G. Escudero, Mat. Sci. Eng. A.**294-296** 388 (2000).
27 [3] J.G. Escudero, Int. J. Mod. Phys. B. **15** 1165 (2001); *ibid* **17** 2789 (2003).
28 [4] J.G. Escudero, Int. J. Mod. Phys. B. **18** 1595 (2004).
29 [5] M. Lachieze-Rey, and J.P. Luminet. Phys. Rep. **254** 136 (1995).
30 [6] J. Levin . Phys Rep. **365** 251 (2002).
31 [7] L.Smolin . How far are we from the quantum theory of gravity, [http://arxiv.org/hep-](http://arxiv.org/hep-th/0303185)
32 [th/0303185](http://arxiv.org/hep-th/0303185) (2003)
33 [8] J.G. Escudero, Chin. J. Astron.Astrophys.**3** 235 (2003)
34 [9] J.G. Escudero, Chin. J. Astron. Astrophys.**4** 343 (2004)
35 [10] F. Pinheiro, et al. Astron.Astrophys.**399** 271 (2003)
36 [11] J.P. Uzan ,R. Lehoucq, and J.P. Luminet, Astron.Astrophys. **351** 766 (1999)
37 [12] M.Trott. *The Mathematica GuideBook for Graphics*.(Springer-Verlag. New York. 2004).
38
39
40
41
42
43
44
45
46
47
48
49
50
51
52
53
54
55
56
57
58
59
60

1
2
3
4
5
6
7
8
9
10
11
12
13
14
15
16
17
18
19
20
21
22
23
24
25
26
27
28
29
30
31
32
33
34
35
36
37
38
39
40
41
42
43
44
45
46
47
48
49
50
51
52
53
54
55
56
57
58
59
60





norm. ampl

freqHcpdL